Proceedings of the ASME 2011 International Mechanical Engineering Congress & Exposition
IMECE2011
November 11-17, 2011, Denver, Colorado, USA

IMECE2011-64706

CURRENT RISE INDEX (CRI) MAPS OF MACHINE TOOL MOTORS FOR TOOL-WEAR PROGNOSTIC

R. F. Hamade
American University of Beirut
Mechanical Engineering Department
P.O. Box 11-0236, Riad El-Solh
Beirut 1107 2020, Lebanon
Email: rh13@aub.edu.lb

A. H. Ammouri
American University of Beirut
Mechanical Engineering Department
P.O. Box 11-0236, Riad El-Solh
Beirut 1107 2020, Lebanon
Email: ahe11@aub.edu.lb

ABSTRACT

Quantitative polar maps of tool-wear of cutting tools (here, chisel drills) undergoing dry machining are charted based only on transducers reporting electrical current measurements from machine (spindle and feed drives) motors. Associated with these maps are qualitative descriptions of the various modes of tool-wear afflicting the drill tools. These tool-wear maps are based a novel wear criterion developed here that relies on the % increase in motor (spindle and feed drive motors) RMS current values and is dubbed the Current Rise Index (CRI). For verification in a drilling operation application, this index is found to positively track the progressive increase in tool-wear.

Utilizing this CRI and the associated polar plots, monitoring of cutting tools may be achieved simply by machine tool operator via visual monitoring of polar CRI maps generated in real-time. Naturally, such plots lend themselves to automated prognosis by common control techniques utilized in machine tool operations. Such maps may also serve as indirect means of predicting tool-wear in automated cutting operations.

1. INTRODUCTION

Wear of cutting tools is an integral part of the machining process since tool condition affects the dimensional accuracy and surface quality of newly machined surfaces. Although most modes of tool wear are progressive in nature, if not replaced, dull tools are likely to fail in a sudden and catastrophic manner causing damage to both work and machine. Therefore, the successful implementation of tool condition monitoring (TCM) becomes critical to the success of fully automated cutting operations. Over the years, many techniques have been used to monitor and detect tool wear in metal cutting in general and, more relevant to this work, in drilling operations. These involve direct as well as indirect measurements of several types of sensors during drilling that correlate to the condition of the tool. While direct measurements rely on visual and computer vision methods to get dimensional values, indirect measurements include a host of techniques including: sonic and ultrasonic vibration/noise detection [1-4], measurements of cutting forces [5-7], and spindle motor / feed drive current measurements [8-11].

For intelligent prediction of tool wear, the artificial neural network, ANN, method is often used. Typically, the network is trained in the first stage where sensor data is fed to the diagnostics software. Once the software has been 'taught' to distinguish a good (sharp) tool from a partially worn one and from a completely dull one, the diagnostic capabilities of the software become automatic resulting in the real-time correct identification of the drilling tool condition by the software. Such an approach has been utilized in [12] where the root mean square (RMS) value of the spindle motor current was used as input to a multilayer neural network.

In this paper, we utilize sensors to instantly measure RMS current of 1) drilling feed drive motor and 2) spindle motor. Further, we establish tracking between these current measurements with corresponding force measurements and, more importantly, with measured tool-wear at various stages of wear. The resulting wear maps are based on a simple measure, dubbed the 'Current Rise Index (CRI)' and which is derived from the increase in RMS current values.

2. EXPERIMENTAL

Two brands of 10mm HSS classic twist drills were used in the study: TERA (Tera Autotech Corporation, No. 1 Industrial Park 7 Rd., Tachia, Taichung Hsien, Taiwan, R.O.C.) and IRWIN (Irwin Tools, 92 Grant Street, Wilmington, OH, USA). Both tool brands were tested and considered for CRI analysis here in order to illustrate the difference between tools of varying quality. The drilled workpiece material was low carbon steel in which 3 mm holes were drilled dry according to the test conditions listed in Table 1. For example, test cell C2 corresponds to spindle speed of 1750 RPM and feed of 0.06 mm/rev, respectively.

TABLE 1: Test matrix showing experimental spindle speeds (RPM) and feeds (mm/rev)

		Feed (mm/rev)			
		0.03	0.06	0.1	0.2
Speed (RPM)	1273	A1	A2	A3	A4
	1592	B1	B2	B3	B4
	1750	C1	C2	C3	C4

Current value measurements were carried out by using hall-effect current transducers that were tapped to individual lines of both the spindle motor and the Z-drive motor of a CNC HAAS VF6 vertical machining center. G-codes were written for each cell in the test matrix. A S22P series current transducer from TAMURA (http://www.tamuracorp.com/clientuploads/pdfs/engineeringdocs/S22PXXXS05.pdf) was used for the spindle motor with a 15A rated current and a LTS6-NP from LEM (http://www.lem.com/hq/en/component/option,com_catalog/task,displaymodel/id,90.37.09.000.0/ was used for the Z-drive motor with a 6A current rating. Both transducers output a 2.5V biased voltage with a 2.5±0.625V full current output voltage.

Signals from the current transducers were acquired by an NI USB-6251 Legacy DAQ device (http://sine.ni.com/nips/cds/view/p/lang/en/nid/209213) into user-friendly LabVIEW software programmed especially for this application. Samples are acquired at a 10K Hz sampling frequency in 2KS batches. The output of the software is raw voltage that represents the cutting cycle current. This raw data is carefully analyzed to extract the RMS of each cutting trial.

2.1 Tool (flank) Wear

As drilling progresses, so do tool wear causing the drill to go from a 'sharp' condition, through a partially worn condition, and ultimately to a dull 'worn out' condition. Catastrophic failures were observed when drilling commenced using dull tools. Wear in drills afflict all regions where metal comes in contact with the drill. However, of the many modes of wear investigated, flank wear, *VB*, is by far the most popular in the metal cutting literature. While many methods exist to quantify flank wear, including taking the average of wear distance at locations along the lip, this work utilizes maximum *VB*, VB_{max}, where the lip meets the margin (at max. cutting speeds [13]).

2.2 Z-Drive Current

While both torque and thrust force progressively increase as the drill tool undergoes wear [7], thrust force has been found to be more sensitive to drill-wear [14]. To eliminate the usage of the expensive (and machine-tool unnatural) force measurement setup, current measurements of the Z-drive motor line are considered. The LTS6-NP current transducer produces real-time current values with a 400 ns response time. A conditioned calibrated signal of the Z-drive current is shown in Figure 1 superimposed on another signal generated from another drilling test in air (test case B3: spindle speed of 1592 RPM and feed of 0.1 mm/rev). The frequency of this particular signal is equal to 3.5 Hz or one full motor cycle = 0.28 s (the value of which depends on the Z-motor driver output for the feed of test case B3 = 0.1 mm/rev). The shown signal corresponds to a tool with drilling history of 7.524 m. Although the two plots are virtually super imposable during the approach stage, significant deviation is recorded during drill engagement. Note that the reason why less current is needed to drive the motor during the drilling stage as compared with during air-drilling is due to the fact that thrust force acts in an opposite direction to tool motion (and gravity). To get a quantitative value of the current, the RMS of the signal is taken into account throughout this paper. In order to remove the bias due to the current consumed from driving the spindle assembly, the RMS is subtracted from the current exerted during air-drill for the same drilling conditions.

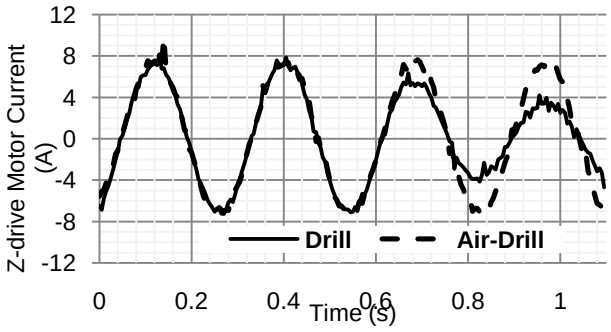

FIGURE 1: Z-drive motor's true current for a typical signal (one full motor cycle = 0.28 second) generated from an actual drilling test superimposed on another corresponding to an air-drilling test (both for the same parameters: test case B3, drilled distance 7.524 m).

2.3 Spindle-Motor Current

Similar to the Z-drive motor, spindle-motor current values were collected by the S22P transducer at a rate of 10 Ks/s. Figure 2 shows a typical example of the collected raw data that corresponds to the same test cell of Figure 1 (B3). As wear progresses, the RMS peak value of the spindle-motor current increases given that the motor draws more current to compensate for additional tool-wear.

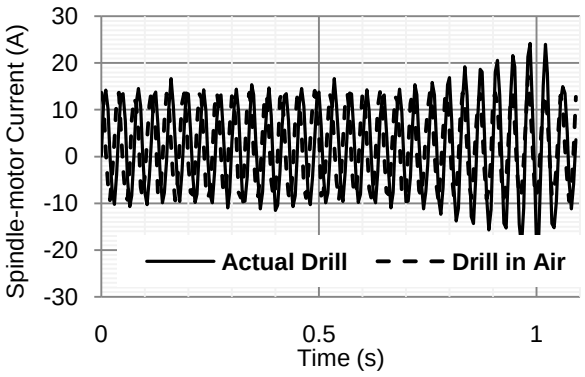

FIGURE 2: Spindle-motor true current for a typical signal (one full motor cycle = 0.28 second) generated from an actual drilling test superimposed on another corresponding to an air-drilling test (both for the same parameters: test case B3, drilled distance 7.524 m).

2.4 Current rise and flank-wear vs. drilled distance

Here we combine the findings of sections 2.1 through 2.4 above. Figure 3 is an example of the measured spindle current (RMS) and Z-drive current (RMS) as well as the progressive wear VB_{max} plotted against the drilled distance (mm) (for a TERA drill, test case C2). Reasonably good tracking is found between current measurements with that of tool-wear where the effect of drill-wear on the spindle motor current can be observed. Similar behavior has been reported (e.g. [15]) for cutting force/torque versus tool-wear for drilling operations.

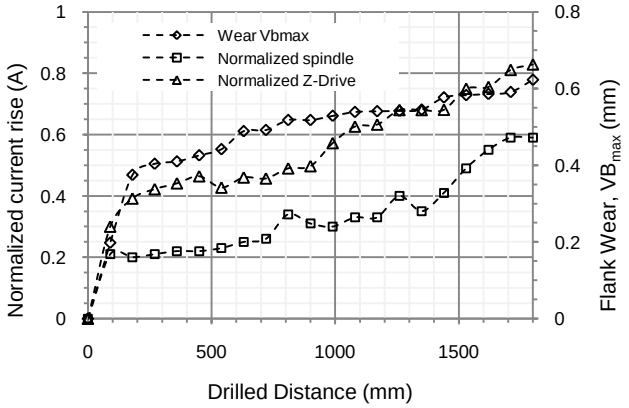

FIGURE 3: Normalized spindle current (RMS) and Z-drive current vs. drilled distance for a TERA drill (test case C2). Progressive flank-wear, VB_{max}, values are also plotted on the secondary axis.

3. THE CURRENT RISE INDEX (CRI) CRITERION

Figure 4 is a linear plot of %rise in the machine tool's spindle and Z drive motors for IRWIN chisel drills (test condition: C3, Table 1: (spindle speed of 1750 RPM and feed of 0.1 mm/rev). One conclusion from the figure is that the thrust feed drive is more sensitive to wear than that of the spindle which exhibits more stability or less % increase as wear (and drilled distance) increases. This is consistent with other works reported for force increase with progressive tool-wear [14].

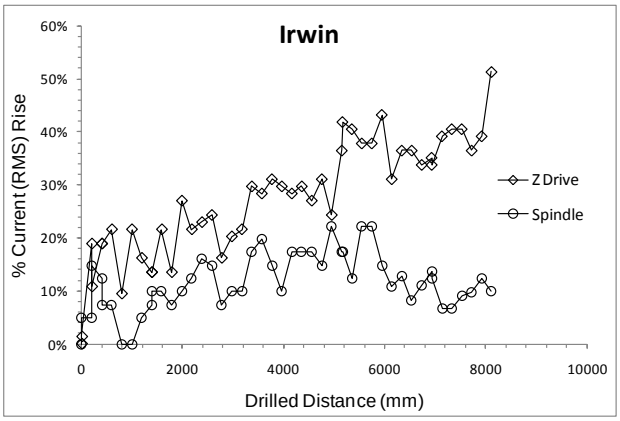

FIGURE 4. Linear plots of % rise in the machine tool's spindle and Z drive motors for IRWIN chisel drills; Test condition: C3.

Re-plotting the % rise in spindle torque versus that of the Z feed drive results in plots such as that in Figure 5 which constitutes the first step towards constructing CRI polar plots.

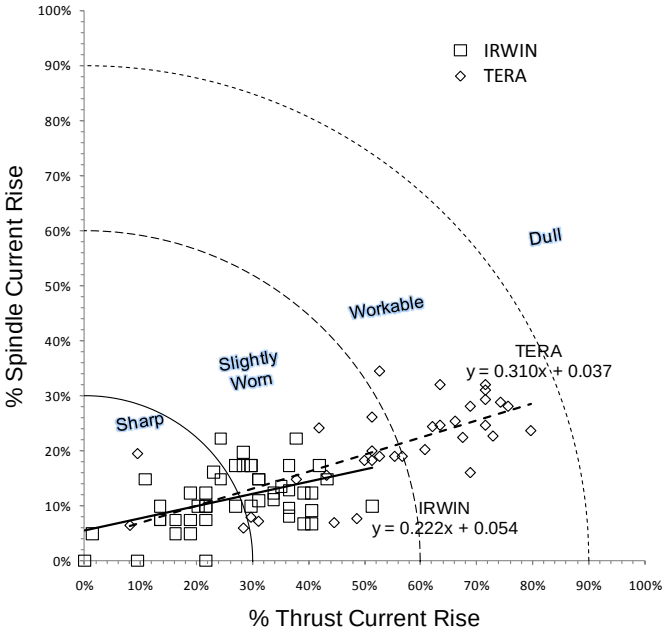

FIGURE 5. Plot of the % rise in spindle torque vs. that of the Z feed drive for test case C3. Drills from both suppliers: IRWIN and TERA.

A direct descendent of the plot in Figure 5 will be the CRI polar plots (such as Figure 7 below) which are based on the following criterion development. A novel representation of progressive tool-wear is based on the acquired data from the current transducer signals. The resulting map is a polar plot based on a measure dubbed here as the Current Rise Index (*CRI*) calculated as the square root of the percent increase in the RMS current values of both transducers. This measure combines both signals in one value that represents the change in current values according to

$$CRI = \sqrt{\Delta I_{Spindle}^{\;2} + \Delta I_{Z-motor}^{\;2}} \qquad (1)$$

Where:

$\Delta I_{Spindle}$ is the % change in spindle motor current

$\Delta I_{Z-motor}$ is the % change in Z-drive motor current

The percentage change in the current signal is found by subtracting the RMS value of the trial being considered from the air-drill RMS value and dividing the result by the RMS value of the first trial as follows

$$\Delta I_i = \frac{I_i - I_1}{I_1 - I_0} \qquad (2)$$

where:

I_i is the RMS value of the test considered

I_0 is the RMS value of the air-drill test

I_1 is the RMS value of the first (wear-free) test

The representation in (2) eliminates the bias of the current signal that comes from the machine dynamics and normalizes the signal such that the first reading is null and the consecutive values are calculated relative to the first trial.

Cutoff CRI ranges in this criterion are not fixed. The range values are adjustable according to the process. The example presented here uses the ranges listed in Table 2. The CRI criterion: CRI ranging from 0-30 % represents a 'sharp' tool condition. CRI ranges from 30-60% and 60-90% represent slightly worn and workable tools, respectively. Tools are considered dull for CRI values grater 90%.

TABLE 2: Example ranges of % current rise for the CRI criterion.

CRI Criterion	
Range	**Tool Condition**
0-30 %	Sharp
30-60%	Slightly Worn
60-90%	Workable
> 90 %	Dull

Applying this CRI criterion to the data in Figure 4 results in Figure 6 which is shows how this criterion may be used in the common linear scale where both the current and spindle change of both drills are plotted on a linear scale along with the CRI vs drilling distance. Combining the input of both motors yields the CRI plot (bottom) for the IRWIN which corresponds to the same drilling data for the tool reported in Figure 4. The 3 horizontal lines represent the criterion's cutoff regions based on 30, 60, and 90% demarcation zones for sharp, slightly worn, and workable too, respectively. The tool is considered in the dull state once the trend-lines (shown on the figure) surpass the workable limit.

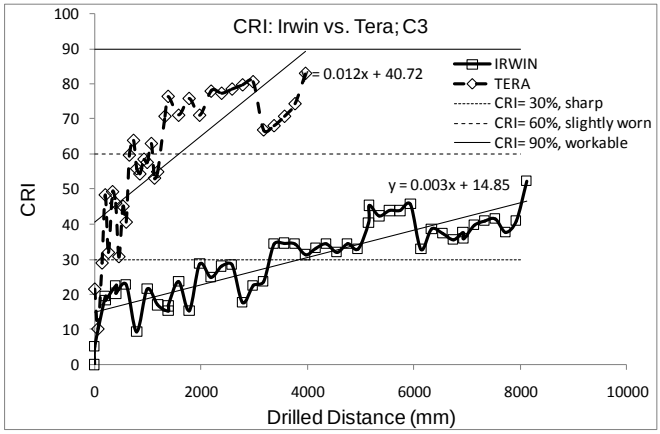

FIGURE 6. Linear plots of CRI tool-wear for drills from TERA and IRWIN; Test condition is C3.

4. POLAR CRI MAPS

A further development involves re-plotting the CRI values in a polar plot format. For example, re-plotting the data previously plotted in Figure 6 in polar form yields Figure 7. This plot represents a typical current rise index (CRI) map.

On a polar wear map, the CRI value and the drilled distance represent the magnitude (*ρ)* and the angle , respectively, of any point plotted. Figure 7 shows such a tool-wear map corresponding to one select cell (C3) from the test matrix (Table 1). Figure 7 compares both the IRWIN and TERA drills for the same cutting cell. The following are observations on how to interpret CRI maps.

The polar wear plot of a desirable tool performance may behave where the *CRI* increases relatively smoothly and gradually with low wear rates as the drilling proceeds. Alternately, a bad performance example is where the *CRI* index increases dramatically after only a few drills. A jerk in a wear-map curve may indicate a sudden breakage in the tool due to a catastrophic failure (or sudden dramatic wear in one of the tool flanks or chisel).

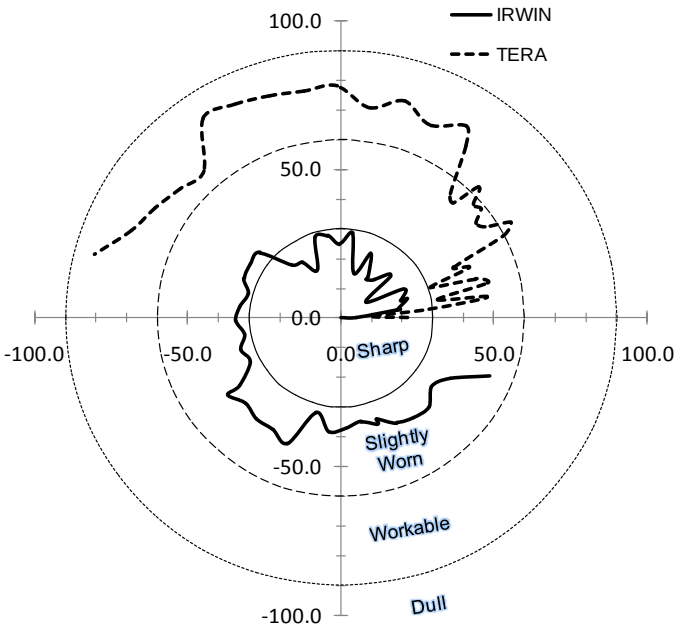

FIGURE 7. Polar plots of CRI tool-wear for drills from both suppliers: TERA and IRWIN; Test conditions: C3.

Polar maps make it easy to compare such measures as the performance of different tools under the same conditions. For example, the fact that the IRWIN drill has gotten ahead of the TERA drill in the angular dimension is indicative of a longer tool life. For case C3, an increased by 50% is seen for the TERA drill on the CRI scale after 220 holes only (0.6m). By comparison, it took IRWIN 2700+ holes (8.1m) to merely cross the same CRI level.

For the sake of completeness, one can attach a tag on the last point on the plot that indicates length. For instance, here each full rotation on the polar plot corresponds to 8.64 meters (or 2880 holes). Such tags will show the same drilled distance as that on the x-axis in Figures 4 and 5.

5. SUMMARY

A novel criterion, dubbed the Current Rise Index (CRI), based only on the combined % increase in the machine tool's spindle and feed motors RMS current values due to tool wear has been presented. Based on this criterion, novel tool wear maps have been introduced which lend themselves to easy decision making by machine operators' visual inspection and monitoring.

These maps can be useful for visual inspection by machine tool operators. They can also be used for sophisticated automation involving decision making purposes where artificial neural networks, ANN, or other AI tools can make correct determinations about the condition of cutting tools.

6. ACKNOWLEDGMENTS

The authors wish to acknowledge the University Research Board (URB) of the American University of Beirut for the financial support of this research. The second author also acknowledges the support of Consolidated Contractors Company through the CCC Doctoral Fellowship in Manufacturing

7. REFERENCES

[1] Mathew, M. T., Srinivasa Pai, P., and L. A. Rocha, 2008, "An effective sensor for tool wear monitoring in face milling: Acoustic emission," 33(3), pp. 227-234.

[2] Schehl, U., 1991, "Werkzeuguberwachung mit Acoustic-Emission beimDrehen", Fra¨sen und Bohren, Aachen.

[3] Hayashi, S. R., Thomas, C.E., and Wildes, D.G., 1998, "Tool break detection by monitoring ultrasonic vibrations," Annals of the CIRP, 37 (1), pp. 61-64.

[4] Kutzner, K., Schehl, U., 1998, "Werkzeuguberwachung von Bohrernkleinen Durchmessers mit Korperschall-sensoren," Industrie Anzeigner 110(82), pp. 32–33.

[5] Lee, K. J. , Lee, T. M., and Yang, M. Y., 2007, "Tool wear monitoring system for CNC end milling using a hybrid approach to cutting force regulation", International Journal Advance Manufacturing Technology, 32, pp. 8-17.

[6] Braun, S., Lenz, E., and Wu, C.L., 1982, "Signature analysis applied to drilling," Journal Mechanical Design, Transactions of the ASME, 104, pp. 268-276.

[7] Lin, S.C., and Ting, C.J., 1995, "Tool wear monitoring in drilling using force signals", Wear 180 (1-2), pp. 53-60.

[8] Jantunen, E., and Jokinen, H., 1996, "Automated On-line Diagnosis of Cutting Tool Condition (Second version)," International Journal of Flexible Automation and Integrated Manufacturing 4 (3-4), pp. 273-287.

[9] Chang, Y.-C., Lee, K.-T., and Chuang, H.-Y. , 1995, "Cutting force estimation of spindle motor," J. Contr. Syst. Technol., 3(2), pp.145-152.

[10] Li, X., 2005, "Development of current sensor for cutting force measurement in turning," IEEE Transactions on Instrumentation and Measurement, 54(1), pp. 289-296.

[11] Noori-Khajavi, A., 1992, "Frequency and time domain analyses of sensor signals in a drilling process and their

correlation with drill wear", PhD Thesis, Oklahoma State University, Stillwater, OK.

[12] Patra, K., Pal, S.K., and Bhattacharyya, K., 2007, "Artificial neural network based prediction of drill flank wear from motor current signals", Applied Soft Computing, 7, pp. 929-935.

[13] Hamade, R. F. Seif, C. Y., and Ismail, F., 2006, "Extracting cutting force coefficients from drilling experiments," International Journal of Machine Tools & Manufacture, 46, pp. 387-396

[14] Oraby, S.E. and Hayhurst, D.R., 2004, "Tool life determination based on the measurement of wear and tool force ratio variation," International Journal of Machine Tools & Manufacture, 44, pp. 1261-126

[15] Hamade, R. F., Manthri, S. P., Pusavec, F., Zacny, K. A., Dillon, O. W. , Rouch, K., and Jawahir, I. S., 2010, "Compact core drilling in basalt rock using rectangular PCD tool inserts: wear characteristics and cutting forces," Journal of Materials Processing Technology, 210 (10), pp. 1326-1339.